Journal of Alloys and Compounds 633 (2015) 120–126

Contents lists available at ScienceDirect

Journal of Alloys and Compounds

journal homepage: www.elsevier.com/locate/jalcom

The effect of Al doping on the crystal structure and magnetocaloric behavior of $Mn_{1.2}Fe_{0.8}P_{1-x}Ge_x$ compounds

D.M. Liu [a,b,*], H. Zhang [a], S.B. Wang [a], W.Q. Xiao [a], Z.L. Zhang [a], N. Tian [a], C.X. Liu [a], M. Yue [b], Q.Z. Huang [c], J.X. Zhang [b], J.W. Lynn [c]

[a] Institute of Microstructure and Property of Advanced Materials, Beijing University of Technology, Beijing 100124, China
[b] Key Laboratory of Advanced Functional Materials, Education Ministry of China, Beijing University of Technology, Beijing 100124, China
[c] NIST Center for Neutron Research, National Institute of Standards and Technology, Gaithersburg, MD 20899, USA

ARTICLE INFO

Article history:
Received 24 September 2014
Received in revised form 16 January 2015
Accepted 21 January 2015
Available online 11 February 2015

Keywords:
Al doping
Magnetocaloric effect
MnFePGe compound

ABSTRACT

We studied the influence of Al doping on the crystal structure and magnetocaloric properties of $Mn_{1.2}Fe_{0.8}P_{1-x}Ge_xAl_y$ compounds prepared by spark plasma sintering, with $x = 0.24$, 0.25, 0.26 and $y = 0$, 0.004, 0.008, 0.010 or 0.12. These compounds have the same Fe_2P-type structure (space group $P\bar{6}2m$) as the undoped system, and we found that the addition of Al had significant effects on the hexagonal unit cell of the compound and its physical properties. As y increased, the lattice parameter a and cell volume increased, the lattice parameter c decreased, the thermal hysteresis (ΔT_{hys}) decreased, and the Curie temperature (T_c) became significantly higher than at $y = 0$. The variations of T_c and ΔT_{hys} correlated almost linearly with variation in the c/a ratio, indicating that T_c can be increased with Al doping. In addition, Al doping did not have any adverse effects on other magnetocaloric properties, such as the entropy change, adiabatic temperature change, and the temperature range of the coexistence of the paramagnetic and ferromagnetic phases. We also found that the magnetocaloric properties of $Mn_{1.2}Fe_{0.8}P_{1-x}Ge_xAl_y$ compounds could be improved by homogenous annealing. The particular composition $Mn_{1.2}Fe_{0.8}P_{0.74}Ge_{0.26}Al_{0.010}$ exhibited a T_c close to room temperature (292.2 K) with a hysteresis of ΔT_{hys} 2.1 K, making it a very promising material for magnetic refrigeration around room temperature.

© 2015 Elsevier B.V. All rights reserved.

1. Introduction

Magnetic refrigeration based on the magnetocaloric effect (MCE) offers a potentially energy saving and environmentally friendly way to replace vapor-compression refrigeration [1,2]. Many new materials with giant MCEs near room temperature have been investigated, e.g. $Gd_5(Si_xGe_{1-x})_4$, $La(Fe_{1-x}Si_x)_{13}$, and $MnFe(P_{1-x}M_x)$ with M = As, Si, or Ge [2–7]. Of these, MnFePGe is one of the most promising candidates for practical applications because it has competitive advantages such as low fabrication costs and environmental benefits. However, to be viable as a practical magnetorefrigerant material, it needs to have a very large MCE under modest applied fields (<2 T), a small hysteresis and magnetostriction, as well as a continuously adjustable T_c near room temperature.

For the MnFePGe system, Trung et al. reported that T_c can be tuned by adjusting the P/Ge ratio or the Mn/Fe ratio [8]. In particular, T_c increases with decreasing Mn content, but the hysteresis also increases; whereas T_c increases approximately linearly with increasing Ge concentration but causes a decrease in the entropy change when $x = 0.25$. Leitão et al. reported that the T_c of the Fe rich side of the $(Mn,Fe)_2(P,Ge)$ system is easy to tune by a careful manipulation of the Fe and Ge content, but the ferro-paramagnetic transition sharpness decreases and the entropy changes for modest fields (under 2 T) becomes very low [9]. Morrison et al. reported that a partial substitution of Al on the Si site of $La(Fe_{0.88}Si_{0.12})_{13}$ can broaden the magnetic transition, but it also causes a decrease in the entropy change, which is an undesirable effect [10]. Wang et al. found that partial substitution of Al for Ga in $Ga_{1-x}Al_xCMn_3$ compounds has the same effect [11]. Guetari et al. found that the T_c of $Pr_2Fe_{17-x}Al_x$ compounds can be shifted to room temperature through compositional engineering [12]. The effect of Al doping on the crystal structure and magnetocaloric behavior of MnFePGe compounds has not been reported so far. In the present study, numbers of Al-doped compounds were prepared. The effect of Al

* Corresponding author at: Institute of Microstructure and Property of Advanced Materials, Beijing University of Technology, Beijing 100124, China.

http://dx.doi.org/10.1016/j.jallcom.2015.01.141
0925-8388/© 2015 Elsevier B.V. All rights reserved.

doping on the crystal structure, magnetic properties, and magnetocaloric behavior of $Mn_{1.2}Fe_{0.8}P_{1-x}Ge_xAl_y$ compounds was investigated.

2. Experimental procedure

$Mn_{1.2}Fe_{0.8}P_{1-x}Ge_xAl_y$ compounds with $x = 0.24$, 0.25, 0.26 and $y = 0.004$, 0.008, 0.010, and 0.12 were prepared by mechanical alloying followed by spark plasma sintering (SPS). Mn (>99.99 wt.%), Fe (>99.99 wt.%), Al (>99.99 wt.%) and red-P (>99.99 wt.%) powders and Ge (>99.9999 wt.%) chips were mixed and ball milled for 1.5 h under an Ar atmosphere in a high energy Pulverisette 4 mill. The as-milled powders were then collected into a carbon mold and fast sintered into a 20 mm diameter cylindrical sample at 1173 K under 30 MPa using the spark plasma sintering technique. Homogenizing annealing of the sintered samples was performed at 1203 K for 72 h. The density of the sample was examined by the Archimedes method. The crystal structures and phase purity of the as-milled powders and the sintered samples were examined using X-ray diffraction (XRD) with Cu Kα radiation, and the data were analyzed by the Rietveld method. SEM (FEI Quanta 200) was used to investigate the microstructure of the compounds. Magnetic measurements were performed in a Quantum Design-VersaLab over the temperature range from 200 to 350 K at interval of 5 K with a maximum magnetic field of 3 T, recorded during field increase and temperature decrease. Calorimetric measurements were carried out in a NETZSCH Instrument DSC 204F by warming and cooling at 5 K/min. The temperature and the enthalpy were calibrated using Indium as a standard. The direct measurement of the adiabatic temperature change was carried out using equipment at the Baotou Research Institute of Rare Earths [13,14].

3. Results and discussion

Fig. 1 shows the XRD patterns of (a) the as-milled powders and (b) the SPS sintered bulk materials, of $Mn_{1.2}Fe_{0.8}P_{0.74}Ge_{0.26}Al_y$. The hexagonal Fe_2P-type crystal structure, space group $P\bar{6}2m$, exists in all the samples with or without Al doping, indicating that the Fe_2P phase formation is not affected by the Al doping. The diffraction peaks of the as-milled powders broadened, indicating that the sizes of the crystallites are very small, but the diffraction peaks of the bulks are sharp and resolution-limited, demonstrating that the crystallites enlarged during the sintering. Very little $Fe_3Mn_4Ge_6$ or MnO impurity phases were found in the bulk samples.

The XRD measurements for the structural analysis were carried out at 323 K, a temperature at which all of the samples were in the paramagnetic phase (PM). The refined crystallographic data for the bulk $Mn_{1.2}Fe_{0.8}P_{1-x}Ge_xAl_y$ are given in Table 1. Fig. 2 shows the lattice parameters, the c/a and the unit-cell volume as a function of Al content. The lattice parameter a increased and the lattice parameter c decreased with increasing Al content, leading to a decrease in the c/a ratio. However, the unit cell volume increased with increasing Al content, demonstrating that the Al had indeed entered the main Fe_2P phase of interest. We noticed that the samples with Al contained fewer impurity phases than the undoped materials.

Fig. 3 shows the backscattered electron SEM images of $Mn_{1.2}Fe_{0.8}P_{0.74}Ge_{0.26}$ and $Mn_{1.2}Fe_{0.8}P_{0.74}Ge_{0.26}Al_{0.010}$. A comparison of the two images shows that overall more pores are present in the sample without Al doping (Fig. 3a), especially inside the grains. This is reflected by a difference in the density of the two samples. Specifically, the sample with Al doping had a greater density (6.7292 g/cm^3) than that in the Al-free sample (6.7044 g/cm^3). Micro-cracks were found in the Al doped sample, but they did not harm the magnetocaloric properties.

Typically MCEs are calculated with the Maxwell relations using magnetization isotherms. But spike-like entropy change curves may come out in the vicinity of the Curie temperature T_c when first-order transitions are present and two phases coexist in the transition process. The equation for calculating ΔS should be modified in such cases [15,16]. In the present alloy system, the strongly first order transition occurs from a paramagnetic (PM) to a ferromagnetic (FM) phase and can be induced either by temperature or by an applied magnetic field. The two phases coexist during the transition process. Our investigation revealed that the two processes exhibit identical evolutions regarding the crystal and magnetic structures, indicating that the entropy changes can be compared [17]. In this study calorimetric measurements with differential scanning calorimetry (DSC) were used to directly measure the latent heat and the entropy change during the temperature induced phase transformation. DSC is also a reliable way to measure the T_c and thermal hysteresis (ΔT_{hys}) associated with the transition. The DSC measurements for these compounds were found to be almost the same whether we used rates of 1 K/min or 5 K/min [17], so we used the more conservative 5 K/min rate in this paper. Fig. 4(a) shows the warming and cooling curves of the bulk $Mn_{1.2}Fe_{0.8}P_{0.74}Ge_{0.26}Al_y$ compounds. For each sample, the endothermic peak in the warming curve and the exothermic peak in the cooling curve indicate the respective temperature of the ferromagnetic (FM)–paramagnetic (PM) phase transitions, i.e. the Curie temperatures of the transitions. The temperature difference between the two peaks is ΔT_{hys}. Fig. 4(b) shows the temperature dependence of the phases transformation entropy S_{DSC} for the compounds. These results were derived from Fig. 4(a) by applying an integral calculation process to each DSC warming and cooling curve.

The interval (ΔT_{coex}) between the starting and ending temperatures of the transition indicates the range (marked in Fig. 4(b)) over which the two phases coexisted. ΔT_{coex} is related to the strength of the external magnetic field required to complete the FM–PM transitions [18] and is used to calculate the phases transformation entropy change $-\Delta S_{DSC}$. A smaller ΔT_{coex} is desirable for practical applications. The magnetocaloric properties derived from the DSC measurements are provided in Table 1.

Fig. 5 shows the variations in T_c, ΔT_{hys}, ΔT_{coex}, and $-\Delta S_{DSC}$ as a function of the Al content for the $Mn_{1.2}Fe_{0.8}P_{0.74}Ge_{0.26}Al_y$ ($y = 0$, 0.004, 0.008, 0.010, 0.012) compounds. By comparing the data for $Mn_{1.2}Fe_{0.8}P_{0.74}Ge_{0.26}Al_y$ in Fig. 5 and Table 1, we found that $y = 0.010$ appears to be the optimal concentration for Al doping. With an increase in Al content from 0 to 0.010, the entropy S_{DSC}

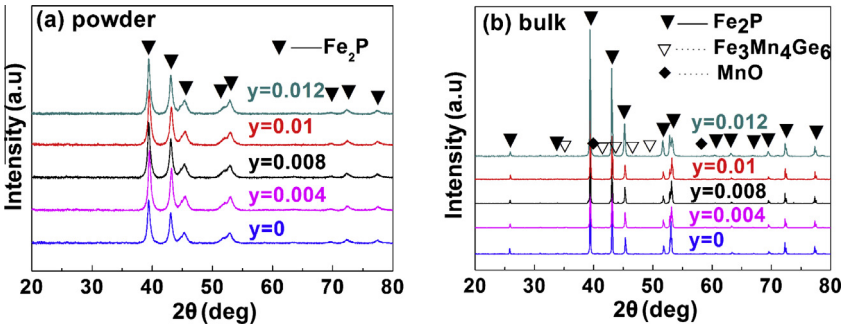

Fig. 1. XRD patterns of (a) the as-milled powders at room-temperature and (b) the sintered bulks of $Mn_{1.2}Fe_{0.8}P_{0.74}Ge_{0.26}Al_y$ at 323 K.

Table 1
Magnetocaloric properties and crystallographic data of bulk $Mn_{1.2}Fe_{0.8}P_{1-x}Ge_xAl_y$ (x = 0.24, 0.25, 0.26; y = 0, 0.004, 0.008, 0.010, 0.012) compounds as a function of Al content.

Sample	T_c (K)	ΔT_{hys} (K)	ΔT_{coex} (K)	$-\Delta S_{DSC}$ (J/kg K)	PMP (%)	Impurity phase (%)	$-*\Delta S_{DSC}$ (J/kg K)	a (Å)	c (Å)	(c/a)	V (Å^3)
#1-$Mn_{1.2}Fe_{0.8}P_{0.74}Ge_{0.26}$	277.4	2.9	9.1	21.5	13.0	2.7	25.4	6.10993(1)	3.45147(2)	0.5649	111.5858(6)
#2-$Mn_{1.2}Fe_{0.8}P_{0.74}Ge_{0.26}Al_{0.004}$	287.2	2.7	8.3	20.8	14.1	1.2	24.5	6.11874(3)	3.44714(2)	0.5634	111.7650(14)
#3-$Mn_{1.2}Fe_{0.8}P_{0.74}Ge_{0.26}Al_{0.008}$	288.6	2.3	10.1	22.1	10.9	1.5	25.2	6.11887(3)	3.44663(1)	0.5633	111.7555(11)
#4-$Mn_{1.2}Fe_{0.8}P_{0.74}Ge_{0.26}Al_{0.010}$	292.2	2.1	9.5	21.2	13.2	1.4	24.7	6.12230(1)	3.44472(7)	0.5627	111.8190(5)
#5-$Mn_{1.2}Fe_{0.8}P_{0.74}Ge_{0.26}Al_{0.012}$	294.4	3.5	18.8	14.4	13.0	1.3	21.9	6.12983(71)	3.44235(5)	0.5616	112.0118(5)
#6-$Mn_{1.2}Fe_{0.8}P_{0.75}Ge_{0.25}$	276.5	3.7	7.1	21.9	20.3	1.6	27.9	6.10508(20)	3.45281(1)	0.5656	111.4517(72)
#7-$Mn_{1.2}Fe_{0.8}P_{0.75}Ge_{0.25}Al_{0.010}$	282.4	3.3	7.3	23.1	14.1	0.9	27.1	6.10896(13)	3.45134(2)	0.5650	111.5461(6)
#8-$Mn_{1.2}Fe_{0.8}P_{0.76}Ge_{0.24}$	260.8	5.4	5.8	21.7	20.9	2.6	28.1	6.09130(5)	3.45730(6)	0.5676	111.0938(30)
#9-$Mn_{1.2}Fe_{0.8}P_{0.76}Ge_{0.24}Al_{0.010}$	271.1	4.9	6.2	21.5	21.1	1.2	27.6	6.09798(13)	3.45460(8)	0.5665	111.2503(55)

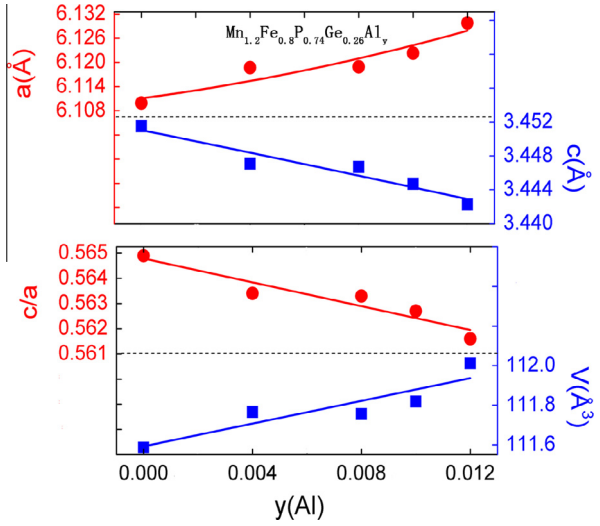

Fig. 2. Variation in the lattice parameters a and c, the c/a, and the unit-cell volume as a function of the Al content for the PM phase at 323 K.

curves shift to higher temperatures, but their values are almost unchanged; T_c increased 14.8 K from 277.4 K to 292.2 K, while the thermal hysteresis ΔT_{hys} decreased from 2.9 to 2.1 K. However, with a further increase to 0.012, the magnetocaloric properties of the compound deteriorated seriously. $-\Delta S_{DSC}$ decreased from 21.2 J/kg K to 14.4 J/kg K, ΔT_{coex} increased from 9.5 K to 18.8 K, ΔT_{hys} increased from 2.1 K to 3.5 K, and T_c increased by 2.2 K. Based on these results, we used 0.010 for the Al doping of $Mn_{1.2}Fe_{0.8}P_{1-x}Ge_x$ (x = 0.25, 0.24) compounds.

Like Fig. 4(b), Fig. 6 shows the temperature dependence of the phases transformation entropy for the $Mn_{1.2}Fe_{0.8}P_{1-x}Ge_xAl_y$ (x = 0.25, 0.24; y = 0 and 0.010) compounds. All the magnetocaloric properties are also given in Table 1. For $Mn_{1.2}Fe_{0.8}P_{0.75}Ge_{0.25}Al_y$ (y = 0, 0.010), $-\Delta S_{DSC}$ increased from 21.9 J/kg K to 23.1 J/kg K, ΔT_{hys} decreased from 3.7 K to 3.4 K, but T_c increased 5.9 K from 276.5 K to 282.4 K. For $Mn_{1.2}Fe_{0.8}P_{0.76}Ge_{0.24}Al_y$ (y = 0, 0.010), $-\Delta S_{DSC}$ was almost the same, ΔT_{hys} decreased from 5.4 K to 4.9 K, T_c increased 10.3 K from 260.8 K to 271.1 K.

Our previous study confirmed that the entropy change is directly related to the FM phase fraction [19], as expected; i.e. a higher FM phase fraction corresponds to a larger entropy change. Because each sample has a different FM phase fraction, a fair comparison of the entropy change $-\Delta S_{DSC}$ has to take this into account. For this reason, a normalized value of the entropy change, $-*\Delta S_{DSC}$, was introduced. In this work, we used the temperature dependent XRD measurement to obtain the FM phase fraction during the FM–PM transition and also calculated the amount of the impurity phase percentage (if any). $-*\Delta S_{DSC}$ can then be normalized from $-\Delta S_{DSC}$ using the following formula:

$$-*\Delta S_{DSC} = \frac{-\Delta S_{DSC}}{(1-\text{PMP}\%)(1-\text{Impurity Phase}\%)}$$

Fig. 7 presents the temperature dependence of the content of the paramagnetic phase percentage calculated from X-ray diffraction for the (a) $Mn_{1.2}Fe_{0.8}P_{0.75}Ge_{0.25}Al_y$ (y = 0, 0.010) and (b) $Mn_{1.2}Fe_{0.8}P_{0.76}Ge_{0.24}Al_y$ (y = 0, 0.010) compounds. The relevant data are given in Table 1. Note that the PM volume fractions in $Mn_{1.2}Fe_{0.8}P_{0.75}Ge_{0.25}$ and $Mn_{1.2}Fe_{0.8}P_{0.75}Ge_{0.25}Al_{0.010}$ at the beginning of the transition were 20.3% and 14.1%, respectively. This means that 6.2% more FM phase was transformed to the PM phase in $Mn_{1.2}Fe_{0.8}P_{0.75}Ge_{0.25}Al_{0.010}$ compared with its undoped counterpart $Mn_{1.2}Fe_{0.8}P_{0.75}Ge_{0.25}$. Because of this increase in the FM phase,

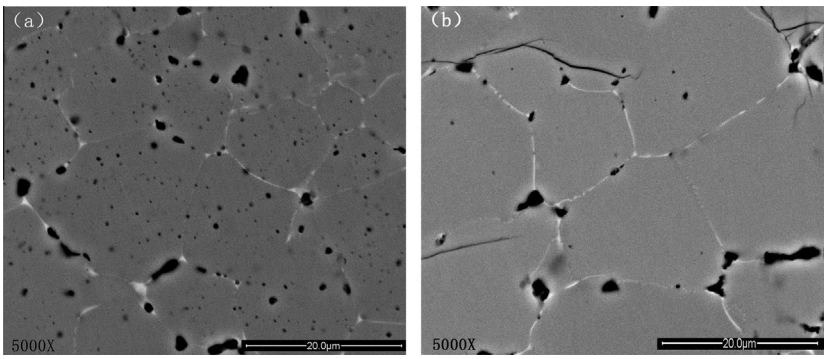

Fig. 3. The BSE images of (a) $Mn_{1.2}Fe_{0.8}P_{0.74}Ge_{0.26}$ and (b) $Mn_{1.2}Fe_{0.8}P_{0.74}Ge_{0.26}Al_{0.010}$.

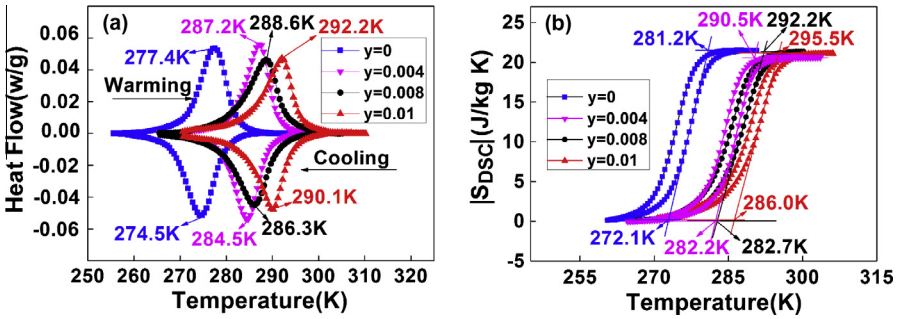

Fig. 4. The warming and cooling curves (a) and the temperature dependence of the PM–FM phases transformation entropy S_{DSC} (b) of the bulk $Mn_{1.2}Fe_{0.8}P_{0.74}Ge_{0.26}Al_y$ (y = 0, 0.004, 0.008, 0.010) compounds.

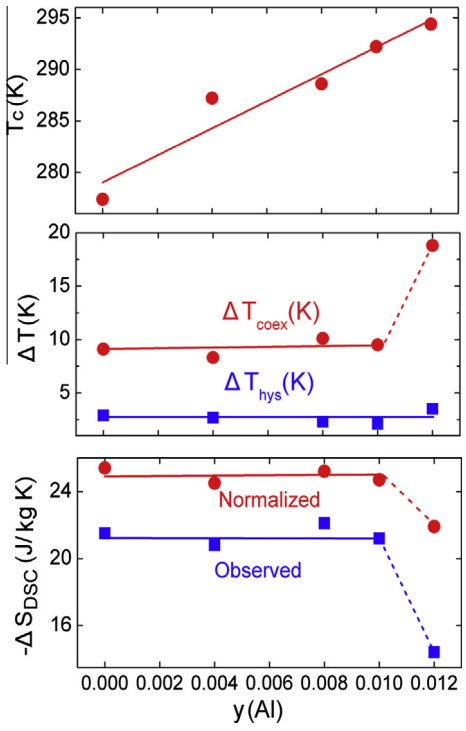

Fig. 5. T_c, ΔT_{hys}, ΔT_{coex} and $-\Delta S_{DSC}$ as a function of Al content for the $Mn_{1.2}Fe_{0.8}P_{0.74}Ge_{0.26}Al_y$ (y = 0, 0.004, 0.008, 0.010, 0.012) compounds.

$-\Delta S_{DSC}$ increased by about 5.5% from 21.9 J/kg K to 23.1 J/kg K, but the values for the normalized $-*\Delta S_{DSC}$ were even closer, i.e. 27.9 J/kg K and 27.1 J/kg K.

The structural refinement results showed that, as the Al content increased, the shape of the unit cell changed and the volume increased, with the smaller c/a ratio resulting in a higher T_c for the compounds, in agreement with previous reports in [8]. In order to demonstrate the effect of variations in c/a on the magnetocaloric properties, the variation in T_c (left axis) and ΔT_{hys} (right axis) as a function of the variation in c/a with the doping of 0.010 Al in $Mn_{1.2}Fe_{0.8}P_{1-x}Ge_xAl_y$ is shown in Fig. 8. As can be seen from the figure, the amount of variation in T_c and ΔT_{hys} corresponded almost linearly with the variation in c/a, i.e. the greater the variation in the c/a ratio, the greater the variation in T_c and ΔT_{hys}.

For $Mn_{1.2}Fe_{0.8}P_{1-x}Ge_x$ (x = 0.24, 0.25, 0.26), Ge acted the same as Al in terms of its effect on the lattice parameters a, c and unit-cell volume. Fig. 9 displays the variations in c/a, T_c, and unit-cell volume (V) as a function of Ge content for the $Mn_{1.2}Fe_{0.8}P_{1-x}Ge_xAl_y$ compounds. This figure shows that, as the c/a ratio decreased with an increase in Ge, the unit cell volume and T_c increased with or without Al doping. Furthermore, Fig. 10 shows the variations in unit-cell volume (V) and T_c as a function of c/a for the $Mn_{1.2}Fe_{0.8}P_{1-x}Ge_xAl_y$ compounds. Compounds with or without Al doping exhibited the same correlations between c/a, unit-cell volume and T_c.

By studying the magnetic exchange interactions in B-, Si-, and As-doped Fe_2P using first-principles theory, Delczeg-Czirjak et al. suggested that doping the P sublattice with elements with fewer valence electrons induces a c/a-ratio decrease which manifests in a T_c increase [20]. Based on our results, we suggest that the Al atoms doped in the $Mn_{1.2}Fe_{0.8}P_{1-x}Ge_xAl_y$ compounds occupy the Ge/P sites in this structure.

In this study, we employed VSM to measure the magnetic properties of the compounds. Isothermal magnetization curves of $Mn_{1.2}Fe_{0.8}P_{0.74}Ge_{0.26}$ and $Mn_{1.2}Fe_{0.8}P_{0.74}Ge_{0.26}Al_{0.008}$ were measured in magnetic fields up to 3 T and the results are presented in Fig. 11. The magnetic entropy changes, $-\Delta S_m$, then can be

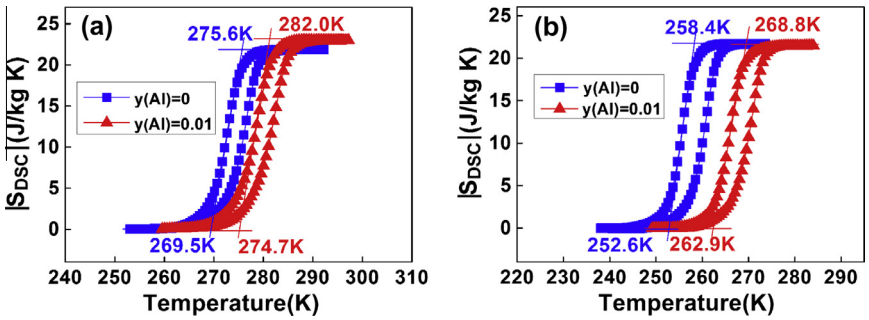

Fig. 6. Temperature dependence of the phases transformation entropy of (a) $Mn_{1.2}Fe_{0.8}P_{0.75}Ge_{0.25}Al_y$ (y = 0, 0.010) and (b) $Mn_{1.2}Fe_{0.8}P_{0.76}Ge_{0.24}Al_y$ (y = 0, 0.010) compounds.

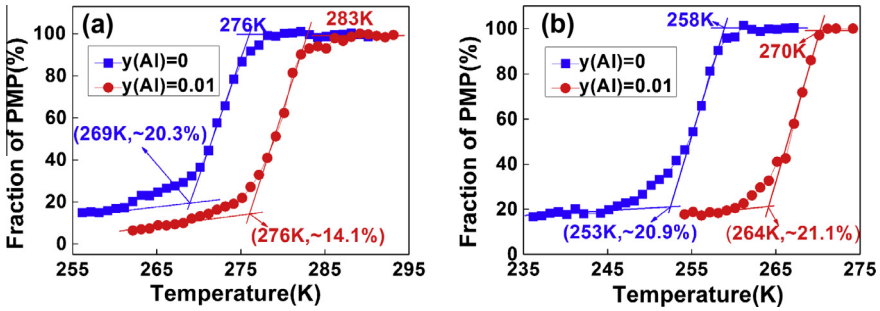

Fig. 7. XRD determination of the phase fraction during the FM to PM transition for the (a) $Mn_{1.2}Fe_{0.8}P_{0.75}Ge_{0.25}Al_y$ (y = 0, 0.010) and (b) $Mn_{1.2}Fe_{0.8}P_{0.76}Ge_{0.24}Al_y$ (y = 0, 0.010) compounds. The measurements were taken during the warming process.

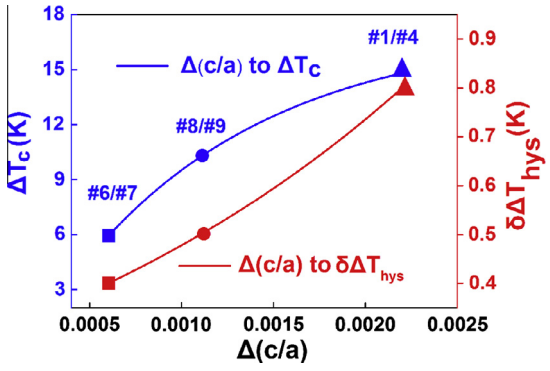

Fig. 8. Increase in T_c (ΔT_c) and decrease in ΔT_{hys} ($\delta\Delta T_{hys}$) vs. decrease in c/a with a doping of 0.010 Al in $Mn_{1.2}Fe_{0.8}P_{1-x}Ge_xAl_y$. The sample reference numbers are given in Table 1.

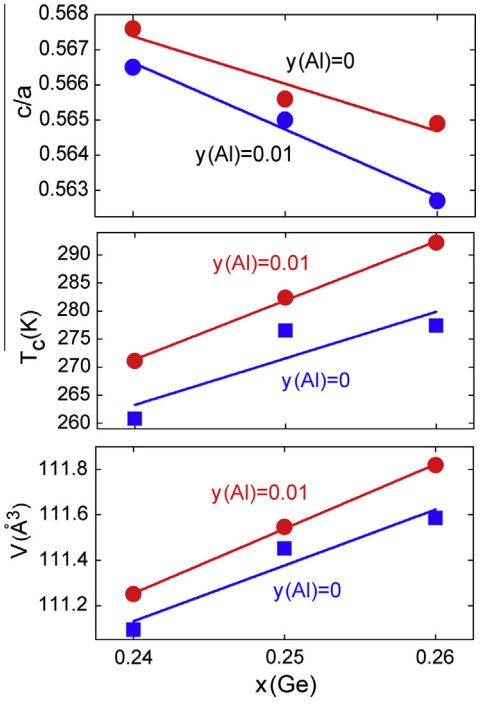

Fig. 9. Variation in c/a, T_c, and unit-cell volume (V) as a function of Ge content for the $Mn_{1.2}Fe_{0.8}P_{1-x}Ge_xAl_y$ compounds (x = 0.24, 0.25, 0.26 and y = 0, 0.010).

obtained using the Maxwell relation. Fig. 12 shows the $-\Delta S_m$ of $Mn_{1.2}Fe_{0.8}P_{1-x}Ge_xAl_y$: (a) ($x$ = 0.26, y = 0, 0.008); (b) (x = 0.24, y = 0, 0.010) compounds as the field changes stepwise from 1 to 3 T. We observed that the magnetic entropy change was essentially unaltered with varying Al content. Both VSM and DSC results show that Al doping did not decrease the entropy change of the MnFePGe compound. Fig. 12(b) also shows that the $-\Delta S_m$ of $Mn_{1.2}Fe_{0.8}P_{0.76}Ge_{0.24}Al_y$ was close to the saturated value for ~2 T near T_c, a finding which indicates that the critical field for the transition is approximately 2 T.

The entropy changes derived from DSC and VSM are related to the FM–PM transitions induced by temperature and magnetic field, respectively. Our previous work showed that, in the MnFePGe system, the crystal and magnetic structures of the FM phases induced by temperature and magnetic field are almost identical; hence, the entropy changes measured from these two methods should be comparable [17]. This was largely true in the present work. For example, for $Mn_{1.2}Fe_{0.8}P_{0.76}Ge_{0.24}Al_{0.010}$ $-\Delta S_m$ was 22.8 J/kg K and $-\Delta S_{DSC}$ was 21.5 J/kg K.

The adiabatic temperature change, ΔT_{ad}, is another important property for a magnetorefrigerant material, and Fig. 13 shows the direct measurement of ΔT_{ad} for $Mn_{1.2}Fe_{0.8}P_{0.76}Ge_{0.24}Al_y$ (y = 0, 0.010) and $Mn_{1.2}Fe_{0.8}P_{0.75}Ge_{0.25}Al_y$ (y = 0, 0.010). The peak of ΔT_{ad}

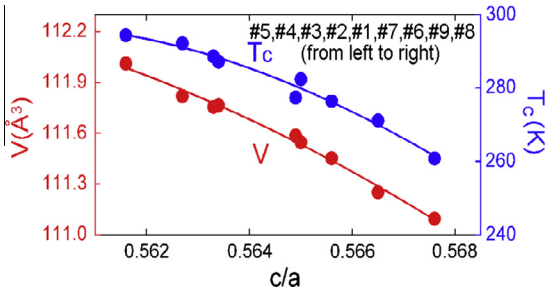

Fig. 10. Variation in unit-cell volume (V) and T_c as a function of c/a for the $Mn_{1.2}Fe_{0.8}P_{1-x}Ge_xAl_y$ compounds (x = 0.24, 0.25, 0.26 and y = 0, 0.004, 0.008, 0.010, 0.012).

shifted to higher temperature (higher T_c) with Al doping, but its value remained at ~2.6 K, indicating that Al doping does not affect ΔT_{ad}.

In our previous study the PM to FM phase transition in the as-sintered sample was incomplete, and the origin of the untransformed PM phase was at least partially due to the small crystallite sizes in the sample. Proper annealing treatments can increase the crystallite size and improve the compositional homogeneity. Here the Al doped compounds were annealed and their magnetocaloric properties were analyzed. Fig. 14 shows the temperature dependence of the entropy of $Mn_{1.2}Fe_{0.8}P_{0.76}Ge_{0.24}Al_{0.010}$ as-sintered and after annealing at 1203 K for 72 h. After annealing, the T_c and ΔT_{hys} were unchanged, but the temperature range of the two-phase coexistence (ΔT_{coex}) decreased from 6.2 K to 4.5 K, a significant improvement of ~27%. At the same time, the entropy change ($-\Delta S_{DSC}$) of $Mn_{1.2}Fe_{0.8}P_{0.76}Ge_{0.24}Al_{0.010}$ increased from 21.5 J/kg K to 23.0 J/kg K, an improvement of ~7%.

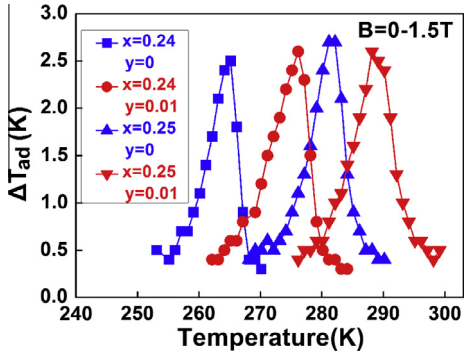

Fig. 13. Temperature dependency of the adiabatic temperature change of $Mn_{1.2}Fe_{0.8}P_{1-x}Ge_xAl_y$ compounds (x = 0.24, 0.25; y = 0, 0.010) in a 1.5 T field.

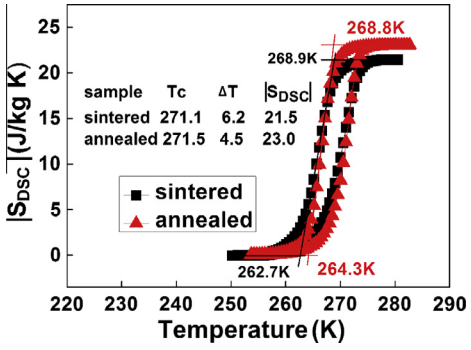

Fig. 14. Temperature dependence of the entropy of $Mn_{1.2}Fe_{0.8}P_{0.76}Ge_{0.24}Al_{0.010}$ as sintered and after annealing.

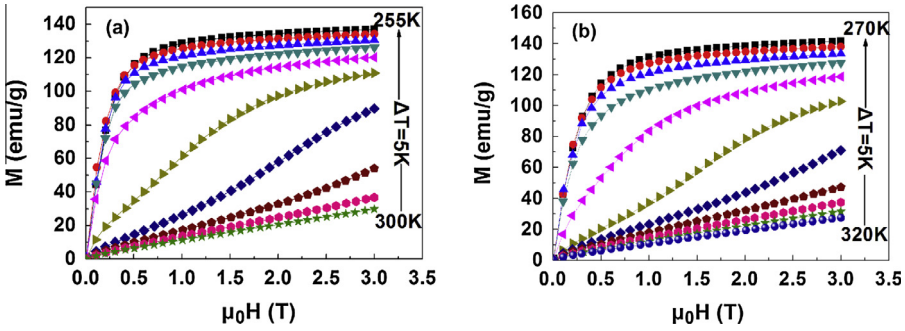

Fig. 11. Isothermal magnetization curves (increasing magnetic field mode) for the (a) $Mn_{1.2}Fe_{0.8}P_{0.74}Ge_{0.26}$; (b) $Mn_{1.2}Fe_{0.8}P_{0.74}Ge_{0.26}Al_{0.008}$ compounds with external magnetic fields of 0–3 T.

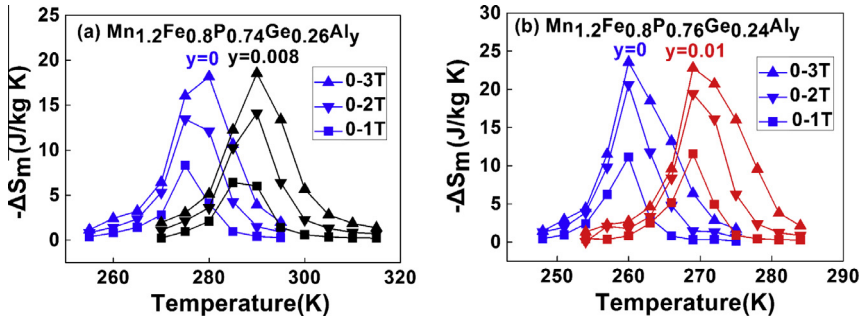

Fig. 12. Temperature dependence of the magnetic entropy changes of the (a) $Mn_{1.2}Fe_{0.8}P_{0.74}Ge_{0.26}Al_y$ (y = 0, 0.008); (b) $Mn_{1.2}Fe_{0.8}P_{0.76}Ge_{0.24}Al_y$ (y = 0, 0.010) compounds measured in a magnetic field of 0, 1, 2 and 3 T.

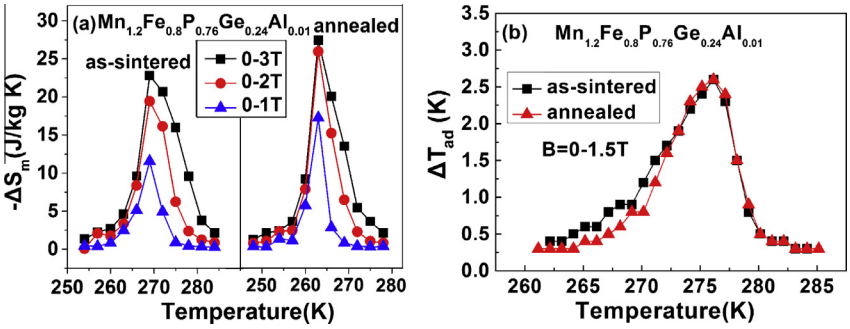

Fig. 15. (a) Temperature dependence of the magnetic entropy change of $Mn_{1.2}Fe_{0.8}P_{0.76}Ge_{0.24}Al_{0.010}$ compounds in the as-sintered and annealed samples measured in a magnetic field of 0, 1, 2 and 3 T; (b) temperature dependency of the adiabatic temperature change of $Mn_{1.2}Fe_{0.8}P_{0.76}Ge_{0.24}Al_{0.010}$ with a field change of 1.5 T.

Fig. 15(a) shows the magnetic entropy change of $Mn_{1.2}Fe_{0.8}P_{0.76}Ge_{0.24}Al_{0.010}$ for the as-sintered and after annealing, measured using the VSM method. The temperature dependence of the adiabatic temperature change is presented in Fig. 15(b), which shows that the magnetic entropy change in the annealed $Mn_{1.2}Fe_{0.8}P_{0.76}Ge_{0.24}Al_{0.010}$ was higher than that in the as-sintered sample. This finding agrees with the DSC result reported in Fig. 14. It also shows that the $-\Delta S_m$ of the annealed $Mn_{1.2}Fe_{0.8}P_{0.76}Ge_{0.24}Al_{0.010}$ was almost fully saturated under 2 T near T_c, but the as-sintered sample was much less so. ΔT_{ad} was about 2.7 K (0–1.5 T) regardless of the heat treatment, as indicated in Fig. 15 (b).

4. Conclusions

Bulk $Mn_{1.2}Fe_{0.8}P_{1-x}Ge_xAl_y$ compounds were prepared through ball milling followed by the SPS method. The effect of Al doping on the crystal structure and magnetocaloric properties were investigated, with the structural analysis suggesting that the Al atoms doped in $Mn_{1.2}Fe_{0.8}P_{1-x}Ge_xAl_y$ compounds occupy the Ge/P sites in the structure. We found that with Al concentrations up to 0.010, c/a decreased, but T_c was higher, and ΔT_{hys} narrowed. The amount of variation in T_c and ΔT_{hys} corresponds almost linearly with variations in c/a. Other magnetocaloric properties, including the entropy change, temperature range of the two-phase coexistence, and adiabatic temperature change, were almost unchanged. This is very important for the practical applications of this system. These results indicate that the Curie temperature of these materials can be increased, with no adverse effect on other magnetocaloric properties. Furthermore, appropriate annealing improves the concomitant magnetocaloric properties of the $Mn_{1.2}Fe_{0.8}P_{1-x}Ge_xAl_y$ system.

Acknowledgments

The authors are grateful to Dr. Antonio Santoro, Dr. Rhoda Edens Perozzi and Dr. Edmund Frank Perozzi for the valuable discussions. The work was supported by the National Natural Science Foundation of China (51071007, 51171003) and the Beijing Natural Science Foundation (KZ201410005005). The identification of any commercial products does not imply endorsement or recommendation by the National Institute of Standards and Technology.

References

[1] J. Glanz, Science 279 (1998) 2045.
[2] K.A. Gschneidner Jr., V.K. Pecharsky, A.O. Tsokol, Rep. Prog. Phys. 68 (2005) 1479.
[3] K.V. Pecharsky, K.A. Gschneidner, Phys. Rev. Lett. 78 (1997) 4494.
[4] F.X. Hu, B.G. Shen, J.R. Sun, Z.H. Cheng, G.H. Rao, X.X. Zhang, Appl. Phys. Lett. 78 (2001) 3675.
[5] T. Mazet, H. Ihou-Mouko, B. Malaman, Appl. Phys. Lett. 89 (2006) 022503.
[6] O. Tegus, E. Brück, K.H.J. Buschow, F.R. de Boer, Nature 415 (2002) 150.
[7] M. Yue, Z.Q. Li, X.B. Liu, H. Xu, D.M. Liu, J.X. Zhang, J. Alloys Comp. 493 (2010) 22.
[8] N.T. Trung, Z.Q. Ou, T.J. Gortenmulder, O. Tegus, K.H.J. Buschow, Appl. Phys. Lett. 94 (2009) 102513.
[9] J.V. Leitão, M. van der Haar, A. Lefering, E. Brück, J. Magn. Magn. Mater. 344 (2013) 49.
[10] K. Morrison, S.M. Podgornykh, Ye.V. Shcherbakova, A.D. Caplin, L.F. Cohen, Phys. Rev. B 83 (2011) 144415.
[11] B.S. Wang, C.C. Li, S. Lin, J.C. Lin, L.J. Li, P. Tong, W.J. Lu, X.B. Zhu, Z.R. Yang, W.H. Song, J.M. Dai, Y.P. Sun, J. Magn. Magn. Mater. 323 (2011) 2017.
[12] R. Guetari, R. Bez, A. Belhadj, K. Zehani, A. Bezergheanu, N. Mliki, L. Bessais, C.B. Cizmas, J. Alloys Comp. 588 (2013) 64.
[13] P.Y. Jin, J.H. Huang, C.L. Liu, F. Guo, J.R. Liu, J.F. Qiu, H.W. Yan, Chin. Rare Earths 28 (2007) 35–38.
[14] Y.X. Geng, O. Tegus, L.G. Bi, Chin. Phys. B 21 (2012) 037504.
[15] J.D. Zou, B.G. Shen, B. Gao, J. Shen, J.R. Sun, Adv. Mater. 21 (2009) 693.
[16] G.J. Liu, S J.R. un, J. Shen, B. Gao, H.W. Zhang, F.X. Hu, B.G. Shen, Appl. Phys. Lett. 90 (2007) 032507.
[17] M. Yue, D.M. Liu, Q.Z. Huang, T. Wang, F.X. Hu, J.B. Li, G.H. Rao, B.G. Shen, J.W. Lynn, J.X. Zhang, J. Appl. Phys. 113 (2013) 043925.
[18] D.M. Liu, Z.L. Zhang, S.L. Zhou, Q.Z. Huang, X.J. Deng, M. Yue, C.X. Liu, F.X. Hu, G.H. Rao, B.G. Shen, J.X. Zhang, J.W. Lynn, Phys. Rev. B (submitted for publication).
[19] D.M. Liu, M. Yue, J.X. Zhang, T.M. McQueen, W.J. Lynn, X.L. Wang, Y. Chen, J. Li, R.J. Cava, X. Liu, Z. Altounian, Q. Huang, Phys. Rev. B 79 (2009) 014435.
[20] E.K. Delczeg-Czirjak, Z. Gercsi, L. Bergqvist, O. Eriksson, L. Szunyogh, P. Nordblad, B. Johansson, L. Vitos, Phys. Rev. B 85 (2012) 224435.